Pergamon

Int. J. Solids Structures Vol. 33, No. 27, pp. 4051–4063, 1996

0020-7683/96 $15.00 + .00

0020-7683(95)00224-3

FURTHER INVESTIGATION FOR THE MACRO–MICROCRACK INTERACTION I—IN THE INFINITE ISOTROPIC BODY

X.-M. WANG, S. GAO, Y.-H. CHEN
Department of Engineering Mechanics, Xian Jiaotong University, Xi'an, Shaanxi, 710049, P.R. China

(*Received* 21 *October* 1994; *in revised form* 4 *September* 1995)

Abstract—This work deals with the problems of the macro–microcrack interaction in an infinite isotropic body. On the basis of the continuously distributed edge dislocation technique and the singular integral equation method which was proved to have higher accuracy and less computation than others treated by previous researchers, the shielding or amplification effect and the so-called neutral angle are re-examined and discussed by using the criterion associated with the mode I stress intensity factor (SIF) and the strain energy release rate (SERR). It is found that there is little difference between the shielding or amplification regions and the neutral positions determined by both criteria when the mode II SIF of a macrocrack is much less than the mode I SIF, but the results from the SERR criterion are completely different from those based on the SIF criterion while the pressure acts on the microcrack, or the remote field phase angle diverges from 90° where the remote field is only dependent on mode I SIF. The simple example is that where, on the basis of the SERR criterion, the microcrack whose centre lies just above the microcrack tip does not always shield the macrocrack when considering the remote field phase angle. In fact, the results from both criteria must be considerably different where the mode II SIF is not small compared to the mode I SIF of the macrocrack, and even takes the dominant place. To some extent, the result from the SERR criterion is more convincing than that from the SIF criterion due to the fact that the SERR can fully characterize the state of the crack tip. Copyright © 1996 Elsevier Science Ltd

1. INTRODUCTION

Since the distributed cracks in an elastic solid have a great impact on the phenomenological behavior of the material, the solution to the problem of a solid with multiple cracks was studied by many researchers and reviewed by Kachanov (1992). Recently, much attention has been paid to the topic where the macrocrack is shielded or antishielded by a transformation strain point and impurity, especially by microcracking within the process zone (Hutchinson, 1987). The model of discrete distributed microcracks around the macrocrack tip is often used to analyse the interaction between macrocrack and microcracks, as the model can be accurately concerned with the orientation, position and size of microcracks (Kachanov and Montagut, 1986; Rose, 1986; Rubinstein, 1985, 1986, 1988; Chudnovsky and Dolgopolsky, 1987a, 1987b; Hori and Nemat-Nasser, 1987; Gong and Horri, 1989; Shum and Hutchinson, 1990). To keep the amount of computation for the model to a tractable level, many approximate methods were suggested, e.g. the iterative-average traction method in which the use of an average traction over each microcrack is introduced (Cai and Faber, 1992), the iterative-point traction approach in which the use of a point-source representation for a microcrack is advanced (Rose, 1986a), the method suggested by Kachanov and Montagut (1986) who used the superposition technique and the idea of self-consistency applied to the average traction on individual cracks, and the method presented by Chudnovsky *et al.* (1987a, b) who adopted the double potential technique with some assumptions. However, all of the approximate methods mentioned above involve some unexamined assumptions or approximations, and their indiscriminate applications probably lead to incorrect conclusions as indicated by Cai and Faber (1992). In view of this fact, the approximate closed-form solution based on the pseudotraction method was derived (Hori and Nemat-Nasser, 1987; Gong and Horii, 1989). Unfortunately, the solution becomes less accurate for the microcrack just above the tip of the macrocrack, and it cannot avoid a tremendous amount of computation if higher accuracy is required.

Similar to the method suggested by Rubinstein and Choi (1988), the technique where the cracks are imitated by the continuously distributed dislocation is recommended to develop the solution for macro–microcrack interaction problems in the present work. The accuracy and efficiency of the solution is fully checked for typical cases of collinear and horizontal microcracks by comparing it with those of the previous works. Then, the shielding or amplification effect of a microcrack on a macrocrack, as well as the neutral angle, is re-examined and discussed by using the criterion concerned with the mode I stress intensity factor (SIF), particularly by applying the alternative criterion bearing on the strain energy release rate (SERR), on account of the fact that all modes should be involved in the characterization of the state of the macrocrack tip. Moreover, the difference between the results on the basis of the two criteria is given, and the effect of the distance from the macrocrack tip to the microcrack center, the remote field phase angle and the traction on the microcrack upon the shielding or amplification of the microcrack are also fully considered.

2. EVALUATION OF THE SOLUTION ACCURACY

Cai and Faber (1992) discussed some approximate methods such as the interative-average traction, the interative-point representation and the method of Kachanov and Montagut for microcrack shielding problems (see Fig. 1). They found that the results could be significantly different from the analytical results or the numerical solution given by the iterative method based on the exact formulation, and meantime presented their applicability ranges in which the errors are acceptably small. As pointed out, those approximate methods are not available any more when the microcrack is very close to the macrocrack. A better solution is the use of the continuously distributed edge dislocation technique and the singular integral equation method which was described by Rubinstein and Choi (1988), formulae for which are derived in more detail in Appendix A.

To discuss fully the accuracy and efficiency of the method combining the distributed edge dislocation technique and singular integral equation, we use the same problems of a collinear microcrack (Fig. 1(a)) and a horizontal microcrack parallel to the macrocrack whose tip is just below the microcrack centre (Fig. 1(b)), as in Cai and Faber (1992). With eqns (A9) and (A10) in mind, the expanded infinite series can be approximated by the interrupted Chebyshev polynominal series with N terms. Then, the SIF of the macrocrack can be calculated (see Appendix A), and shown as in Fig. 2 for collinear microcrack case or Fig. 3 for the horizontal microcrack case. The results for the collinear microcrack show that the solution of $N = 6$ agrees with the analytical and numerical results given by Cai and Faber when $L/2a \geqslant 0.0875$, where the error is less than 1%. Moreover, the solution of $N = 10$ is the same as the analytical results given by Rubinstein (1985), Cai and Faber, or Rose (1986b). In addition, as depicted in Fig. 3 for the horizontal microcrack, all solutions of SIF are acceptable while $H/2a \geqslant 0.125$ for $N = 6$, $H/2a \geqslant 0.1$ for $N = 10$, $H/2a \geqslant 0.075$ for $N = 14$, $H/2a \geqslant 0.0625$ for $N = 18$ and $H/2a \geqslant 0.05$ for $N = 22$, and the largest difference is less than about 6% compared to the numerical results from Cai and Faber. The results for $H/2a \leqslant 0.2$ are tabulated in Table 1.

Compared to the methods discussed by Cai and Faber (1992) and one presented by Gong and Horii (1989), the solution applied in this paper displays much higher accuracy with less computation and simpler formulae. From a theoretical viewpoint, the solution

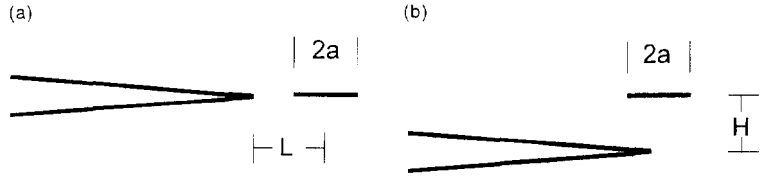

Fig. 1. The macrocrack and microcrack configurations used to discuss the accuracy of the solution. (a) The collinear microcrack. (b) The horizontal microcrack.

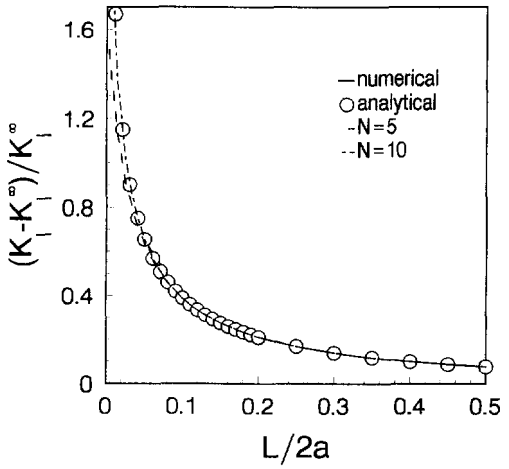

Fig. 2. Comparison of stress intensity factor between the analytical, numerical solution (Cai and Faber, 1992; Rubinstein, 1985; Rose, 1986b) and the results of $N = 5, 10$ for the collinear microcrack. N is the number of interrupted series of the Chebyshev polynominal.

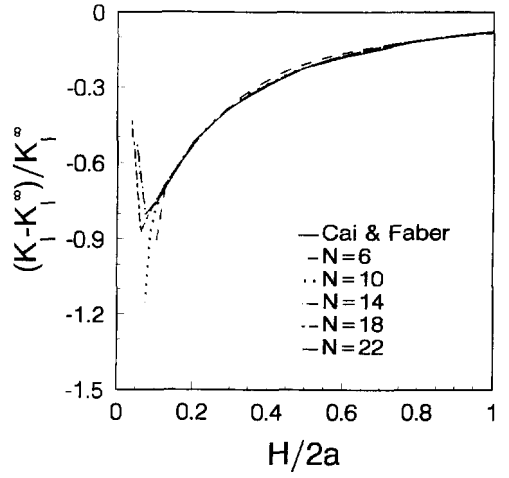

Fig. 3. Comparison of the stress intensity factor between the numerical solution (Cai and Faber, 1992) and the result of $N = 6, 10, 14, 18, 22$ for the horizontal microcrack. N is the number of the interrupted series of the Chebyshev polynominal.

Table 1. The evaluation of accuracy of $(K_I - K_I')/K_I'$ when $H/2a \leqslant 0.2$

$H/2a$	0.0500	0.0625	0.0750	0.1000	0.1250	0.1500	0.2000
Cai and Faber	—	—	—	−0.77	−0.67	−0.62	−0.52
$N = 6$	—	—	—	—	−0.709	−0.635	−0.536
$N = 10$	—	—	—	−0.790	−0.699	−0.636	−0.530
$N = 14$	—	—	−0.803	−0.753	−0.692	−0.633	−0.531
$N = 18$	—	−0.876	−0.829	−0.757	−0.693	−0.634	−0.533
$N = 22$	−0.951	−0.864	−0.826	−0.758	−0.694	−0.635	−0.534

accuracy is restricted by the number of the interrupted series of the Chebyshev polynominal but not by the method presented in Appendix A, and highly accurate results are obtained only by choosing a greater number of terms of the interrupted series since the derived solution is based on the exact analytical formulation without any unexamined assumptions other than the supposition that all cracks are open. This view has been partially confirmed from Table 1.

In addition, as listed in Table 1, to keep the results within acceptable accuracy, the number of the interrupted series must equal 10 and $H/2a$ must be greater than 0.2. Therefore $N = 10$ will be used in the following calculation.

3. INFLUENCE OF SOME FACTORS ON MICROCRACK SHIELDING AND AMPLIFICATION

For the problems of the macro–microcrack interaction, the neutral position is located where the change from the case that the microcrack amplifies the macrocrack to the case that microcrack shields the macrocrack takes place, and its polar angle is named the neutral angle for the specified polar radius. Following from this definition, the criterion to determine the neutral position is described as one where the microcrack with the specified orientation and length is given by:

$$\omega_K = K_I/K_I^{\infty} = 1 \tag{1a}$$

or

$$\omega_G = G/G^{\infty} = 1 \tag{1b}$$

where K_I, G denotes the SIF of the macrocrack and the relevant SERR, respectively, K_I^{∞} and G^{∞} are the SIF and relevant SERR to describe the remote field, ω_K or $\omega_G < 1$ implies that the microcrack shields the macrocrack and ω_K or $\omega_G > 1$ signifies that the microcrack amplifies the macrocrack. Equations (1a) and (1b) might as well be named the SIF criterion and the SERR criterion.

Clearly, the neutral position is the most important parameter of macro–microcrack interaction, and it will be involved in all the following discussions including the regions of microcrack shielding and amplification.

As a prototype, only one microcrack in the process zone of the macrocrack is considered (Fig. A2) in this section, and the subscript k of the variables associated with the microcrack is omitted. Furthermore, it is supposed that the microcrack faces are always free of the traction unless it is specified.

Distance from microcrack centre to macrocrack tip

On account of the SIF criterion (1a) and the distance designated by d from the microcrack centre to the macrocrack tip, the neutral angles for the parallel microcrack ($\varphi = 0$) are calculated and listed in Table 2(a). They increase continuously with d/a, and the result for $d/a = 1.5$ conforms to the prediction of Rubinstein (1986) and Gong *et al.* (1989).

Table 2. The neutral angle θ and K_{II}: K_I for parallel microcrack ($\phi = 0$)

(a) on the basis of the criterion (1a)

d/a	1.1	1.5	2.0	3.0
θ	56.72	62.84	65.94	68.21
K_{II}: K_I%	22.07	14.30	9.04	4.43

(b) on the basis of the criterion (1b)

d/a	1.1	1.5	2.0	3.0
θ	59.66	64.51	66.93	68.61

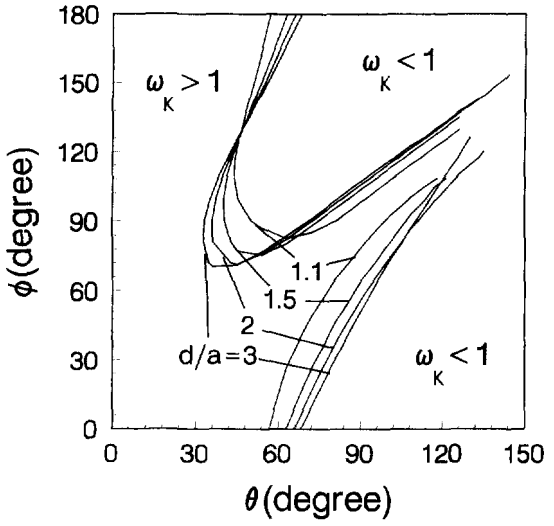

Fig. 4. The illustration of the shielding and amplification regions for $d/a = 1.1$, 1.5, 2.0 and 3.0, determined by $\omega_K = 1$.

Figure 4 illustrates the regions of shielding and amplification with respect to the position angle θ and microcrack orientation φ concerning $d/a = 1.1$, 1.5, 2.0 and 3.0. The neutral angle lines of $K_I^{ma}/K_I^{\infty} = 1$ are seen to cross at $\varphi = 135°$, $\theta = 45°$, which hints that the neutral angle ($\theta \approx 45°$) is weakly dependent on the distance between the microcrack centre and the macrocrack tip for the specified microcrack orientation $\varphi \approx 135°$. In addition, Fig. 5 shows that d/a has a profound influence on the gradient of K_I^{ma}/K_I^{∞} with respect to the position angle θ and microcrack orientation φ.

As previously known, K_I^{ma} is inclined to K_I^{∞} as the distance $d \to \infty$. The subtraction of the minimum of SIF K_{Imin} from the maximum K_{Imax} for a distance d tends to zero. As a result, the parameter defined as $(K_{Imax} - K_{Imin})/K_I^{\infty}$ can be applied to describe the degree of macro–microcrack interaction. As shown in Fig. 6, the parameter decreases to 1.8% as $d/a = 7$. If the 5% error of the parameter is acceptable, the interaction can be ignored as d/a is greater than 4.1.

Mode II stress intensity factor

As previously known, not only mode I SIF K_I but also mode II SIF K_{II} are needed in order to fully characterize the state of the crack tip for in-plane deformation, and therefore the application of the SERR, including all modes, to the analyses of the neutral angle of

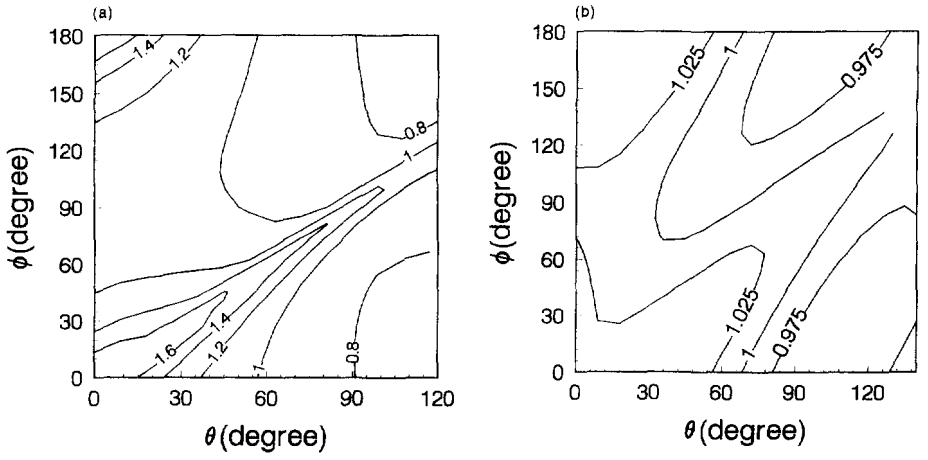

Fig. 5. The topography of ω_K for: (a) $d/a = 1.1$, (b) $d/a = 3.0$.

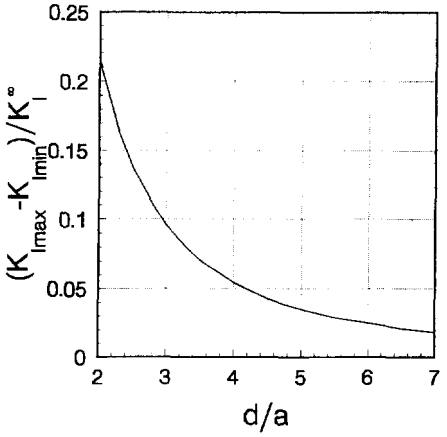

Fig. 6. The shielding or amplification effect of a parallel microcrack on the macrocrack with respect to d/a.

the macro–microcrack interaction is essential for the theoretical viewpoint. The determination of the neutral angle with the SERR criterion (1b) is also required. It is certain that the value of the neutral angle from eqn (1b) must be different from that given by the SIF criterion eqn (1a). For instance, the neutral angle is 62.8° for a parallel microcrack of $d/a = 1.5$ (listed in Table 1(a)), but 64.5° (listed in Table 2(b)) for the same problem if eqn (1b) is applied. Other results are tabulated in Table 2 from which it is found that the neutral angles estimated by eqn (1b) are always greater than those estimated by eqn (1a), and the difference between the results becomes less and less with the increase of d/a or the decrease of K_{II}/K_I. Moreover, Table 2 demonstrates that the application of either the SIF criterion or the SERR criterion to determine the neutral angle is approximately synonymous when K_{II}/K_I is less than about 25% (5% error is allowed). Furthermore, Fig. 7 displays the small difference between the regions of shielding and amplification from eqn (1a) and (1b) when K_{II}/K_I is quite small.

It is concluded that the mode II SIF of the macrocrack must have an impact on the neutral angle, so long as the SERR criterion is adopted, even though the remote field is determined only by mode I SIF. So, given that the aim is to recognize the macro–microcrack interaction completely, the SERR criterion should be adopted unless K_{II}/K_I is less than about 25%.

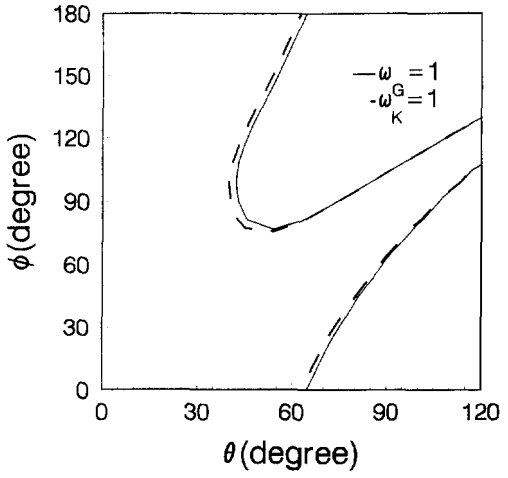

Fig. 7. Comparison of the regions of shielding and amplification between $\omega_G = 1$ and $\omega_K = 1$ for $d/a = 1.5$.

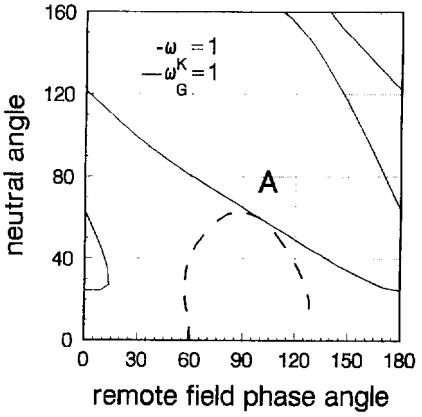

Fig. 8. The neutral angle with respect to the remote field phase angle for $d/a = 1.5$, determined by $\omega_K = 1$ (dashed line) and $\omega_G = 1$ (solid line).

Mixed mode of the remote field

In previous works, the remote field has always been determined by mode I SIF. It simplifies the problem of macro–microcrack interaction, but it probably loses some important information. Thus, we will now consider the mixed mode of the remote field, where the remote field phase angle is defined as

$$\psi = \tan^{-1}(K_I^r / K_{II}^r) \tag{2}$$

where K_{II}^r and K_I^r represent the SIF to determine the remote field.

Considering the greater than normal accuracy required, we calculated the neutral angle for the parallel microcrack, with respect to the remote field phase angle, from 0° to 180° on the basis of both the SIF and the SERR criterion (1a, b) (see Fig. 8), and found that, not only does the neutral angle become multivalued for most of the range, but also the results from eqn (1a) and (1b) are completely different to each other apart from one point A near $\psi = 90°$ where the same prediction of the neutral angle is obtained from eqn (1a) and (1b). It is worth mentioning that the neutral angle in Fig. 8 is not always less than 90°. This implies that the microcrack whose centre lies horizontally above the macrocrack tip (see Fig. 1b) does not always shield the macrocrack. On the contrary, the microcrack amplifies the macrocrack when K_{II}^r is dominant for ψ near 0° or 180°. This is a quite different result from that under the consideration of criterion (1a) as usual.

In the light of what has been discussed in the above section, the SERR criterion (1b) will be used to determine the regions of microcrack shielding or amplification. Shown in Fig. 9(a), it illustrates the regions for $\psi = 90°$ and 45°, respectively, and demonstrates that

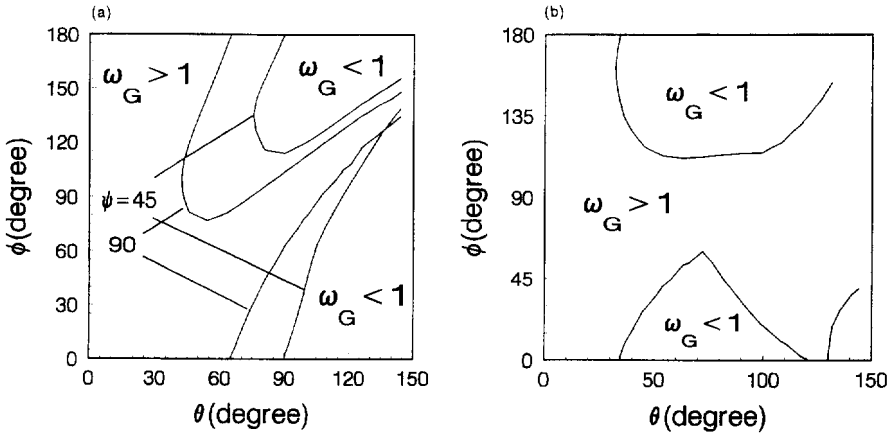

Fig. 9. The regions of shielding and amplification for the remote field phase angle (a) $\psi = 45°, 90°$, (b) $\psi = 150°$, determined by $\omega_G = 1$.

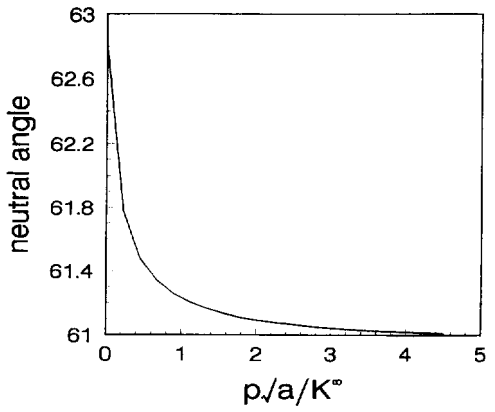

Fig. 10. The neutral angle with respect to pressure upon a parallel microcrack for $d/a = 1.5$, determined by $\omega_K = 1$.

the regions are distinctly dependent on the remote field phase angle. In addition, the shielding regions seem smaller with respect to the smaller ψ. Nevertheless, three shielding regions for ψ near 0° or 180° are found while ψ varies from 0° to 180°, and an example is depicted as in Fig. 9(b), where $\psi = 150$.

Clearly, the interaction of macro–microcrack becomes more complicated when the mixed mode of the remote field is involved, even if only one microcrack is assumed to lie in the process zone. On account of the fact that the K_{II} of the macrocrack gradually takes the prevailing place when ψ diverges from 90°, the discussion of the micro–macrocrack interaction with only mode I SIF is deficient and even misleading.

Traction on the microcrack

So far, the microcrack faces have been assumed to be free of traction. It is necessary to take the traction into account, for instance, when the media is saturated with some liquid or gas, or the residual stress is released by microcracking. Consequently, the microcrack subjected to pressure is assumed in the following.

Firstly, the neutral angles for the parallel microcrack and the regions of shielding and amplification are calculated on the basis of the SIF criterion (1a), shown in Figs 10 and 11, respectively. Both figures show that the angles and regions seem weakly dependent on the pressure put on the microcrack, but such results are not real because K_{II} is not affected, but whilst it closely relies on the pressure and has the same order as K_I, it may even take the dominant part.

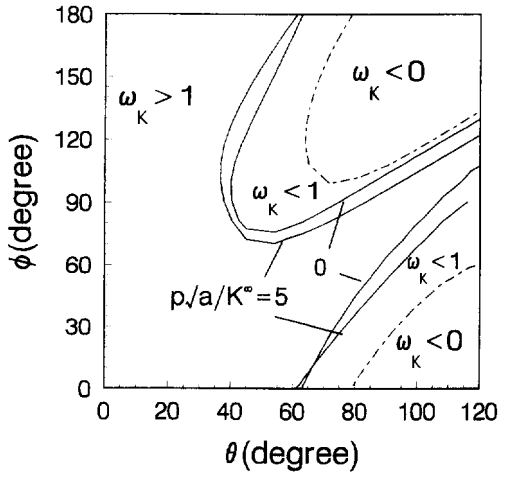

Fig. 11. The regions of shielding and amplification as pressure $p\sqrt{a}/K_I = 0.0$ and 5.0, $d/a = 1.5$, determined by $\omega_K = 1$.

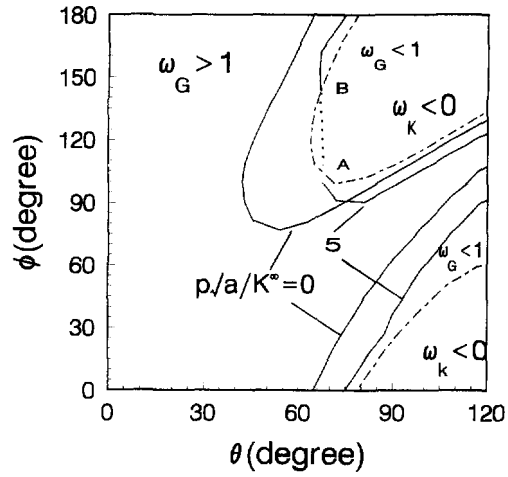

Fig. 12. The regions of shielding and amplification as pressure $p\sqrt{a}/K_I^\infty = 0.0$ and 5.0, $d/a = 1.5$, determined by $\omega_G = 1$.

Table 3. The neutral angle on the criterion (1b) for parallel microcrack subjected to pressure, $d/a = 1.5$

$p\sqrt{a}/K_I^\infty$	0.0	0.4	0.8	1.2	1.6	2.0	2.4
θ	64.5	64.9	66.2	67.8	69.8	72.4	76.1

It is also noted that a phenomenon where $\omega_K < 0$ within the region enclosed by the dash and dot line (see Fig. 11) is found, implies $K_I < 0$ and signifies the macrocrack tip closing. Because the derived formulation is based on the supposition that the microcrack is always open, all results for $K_I < 0$ are distorted.

Shown in Fig. 12, the regions of shielding and amplification are calculated with the SERR criterion (1b) and are clearly dependent upon the pressure on the microcrack. Due to the distortion of the results within the region of $\omega_K < 0$, the neutral line shown by the imaginary dotted line AB is missing. Furthermore, the neutral angles for the parallel microcrack are again calculated on the basis of eqn (1b) and listed as in Table 3. They completely diverge from the results based on eqn (1a). The reason is that the K_{II} of the macrocrack acts in a more and more significant role in the macro–microcrack interaction.

4. CONCLUSIONS

By simulating the macrocrack and microcracks with arrays of distributed edge dislocations for the macro–microcrack interaction of in-plane deformation, the numerical results for the collinear and horizontal microcracks are calculated and display a much higher accuracy with less computation. The discussion shows that the distance from the microcrack centre to the macrocrack tip has an influence on the neutral position and the regions of shielding and amplification, and when it reaches four times greater than half a length of the microcrack the interaction between the macrocrack and microcrack can be approximately ignored. Further discussion shows that the position and the regions predicted by the SIF criterion change more or less when the mode II SIF of the macrocrack is involved and the SERR criterion is applied. In particular, both criteria lead to a completely different prediction if the mode II SIF is not considerably smaller than the mode I SIF and even takes the dominant place.

In view of the fact that the SERR is consistent in all modes of the macrocrack tip, the results based on the SERR criterion is more convincing than those based on the SIF criterion. With the SERR criterion, the neutral position appears to be multivalued and the regions of microcrack shielding become more complicated when the mixed mode of the remote field is considered, meanwhile the position and the regions are also closely reliant

on the pressure on the microcrack. Moreover, it is displayed that the position and the regions are distinct from ones estimated by the SIF criterion.

Acknowledgement—This work was supported by the Foundation of The State Key Laboratory of Mechanical Structural Strength and Vibration. The authors are deeply grateful to Prof. Y.-P. Shen for his help.

REFERENCES

Cai H. and Faber K. T. (1992). On the use of approximation methods for microcrack shielding problems. *J. Appl. Mech. ASME* **59,** 497–501.
Chudnovsky, A., Dolgopolsky, A. and Kachanov, M. (1987a). Elastic interaction of a crack with a microcrack array. I—formulation of the problem and general form of the solution. *Int. J. Solids Structures* **23,** 1–10.
Chudnovsky, A., Dolgopolsky, A. and Kachanov, M. (1987b). Elastic interaction of a crack with a microcrack array. II—elastic solution for two crack configurations. *Int. J. Solids Structures* **23,** 11–21.
Erdogan, F., Gupta, G. D. and Cook, T. S. (1973). Numerical solution of singular integral equations. In *Methods of Analysis and Solution of Crack Problems. Mechanics of Fracture* (ed. G. C. Sih), Vol. 1, pp. 368–345.
Gong, S.-X. and Horii, H. (1989). General solution to the problem of microcrack near the tip of a main crack. *J. Mech. Phys. Solids* **37,** 27–46.
Hori, M. and Nemat-Nasser, S. (1987). Interacting micro-cracks near the tip in the process zone of a macro-crack. *J. Mech. Phys. Solids* **35,** 601–629.
Hutchinson, J. W. (1987). Crack tip shielding by micro-cracking in brittle solids. *Acta Metallica* **35,** 1605–1619.
Hutchinson, J. W., Mear, M. E. and Rice, J. R. (1987). Crack paralleling an interface between dissimilar material. *J. Appl. Mech. ASME* **54,** 828–832.
Kachanov, M. and Montagut, E. (1986). Interaction of a crack with certain microcracks arrays. *Engng Fract. Mech.* **25,** 625–636.
Kachanov, M. (1992). Effective elastic properties of cracked solid: critical reviews of some basic concepts. *Appl. Mech. Rev.* **15,** 304–335.
Muskhelishvili, N. I. (1953). *Some Basic Problems of the Mathematical Theory of Elasticity*. Nordhoff, Holland.
Rose, L. R. F. (1986a). Microcrack interaction with main crack. *Int. J. Fract.* **31,** 233–242.
Rose, L. R. F. (1986b). Effective fracture toughness of microcracked materials. *J. Am. Ceram. Soc.* **69,** 212–214.
Rubinstein, A. A. (1985). Macrocrack interaction with semi-infinite microcrack arrays. *Int. J. Fract.* **27,** 113–119.
Rubinstein, A. A. (1986). Macrocrack-microdefect interaction. *J. Appl. Mech. ASME* **53,** 505–510.
Rubinstein, A. A. and Choi, H. C. (1988). Macrocrack interaction with transverse array of microcracks. *Int. J. Fract.* **36,** 15–26.
Shum, D. K. M. and Hutchinson, J. W. (1990). On toughening by microcracks. *Mech. of Mater.* **9,** 83–91.
Suo, Z. (1989). Singularities interacting with interface and cracks. *Int. J. Solids Structures* **25,** 1133–1142.

APPENDIX A. FORMULATION AND SOLUTION

In terms of the complex potential $\Phi(z)$ and $\Omega(z)$ for plane elasticity (Muskhelishvili, 1953), the stress and displacement components are

$$\sigma_{xx}+\sigma_{yy}=2[\Phi(z)+\overline{\Phi(z)}] \quad \sigma_{yy}-i\sigma_{xy}=\overline{\Phi(z)}+\Omega(z)+(\bar{z}-z)\Phi'(z)$$
$$2\mu\frac{\partial}{\partial x}(u_x-iu_y)=\kappa\overline{\Phi(z)}-\Omega(z)-(\bar{z}-z)\Phi'(z) \tag{A1}$$

For the edge dislocation in an infinite body, shown as in Fig. A1, $\Phi(z)$ and $\Omega(z)$ are put in the following forms (Suo, 1989)

$$\Phi_0(z)=B\left(\frac{1}{z-s}\right), \quad \Omega_0(z)=B\left[\frac{\bar{s}-s}{(z-s)^2}\right]+\bar{B}\left(\frac{1}{z-s}\right) \quad B=\frac{\mu}{\pi i(1+\kappa)}(b_x+ib_y) \tag{A2}$$

where b_x and b_y are the two components of edge discloation, and μ is the shear modulus, $\kappa=3-4\nu$ for plane strain and $(3-\nu)/(1+\nu)$ for plane stress.

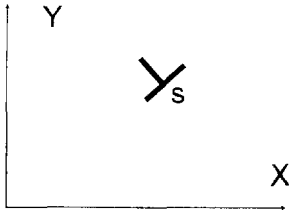

Fig. A1. The edge dislocation in an infinite body.

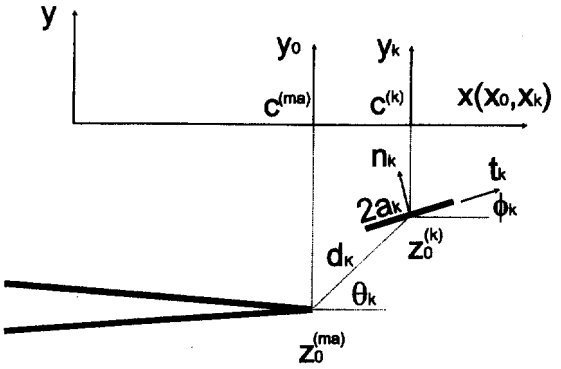

Fig. A2. The configuration of a macrocrack and a k-th microcrack.

In the present case, it is considered that the problem of an infinite body containing a macrocrack is described as a semi-infinite crack and a set of microcracks of length $2a_k$, $k = 1, \ldots, M$, shown as in Fig. A2. With respect to the rectangular Cartesian coordinate system (X, Y), the local coordinates (X_0, Y_0) with the origin $Z_0^{(ma)}$ at the tip of the macrocrack and (X_k, Y_k) with the origin $Z_0^{(k)}$ at the center of the k-th microcrack are employed, and their horizontal translations are $C^{(ma)}$ and $C^{(k)}$ respectively. The normal and tangent direction of the microcrack are denoted by n_k and t_k, the position angle and the orientation of microcrack are designated by θ_k, φ_k, and the distance from the macrocrack tip to the centre of the microcrack is d_k.

Simulating the macrocrack and a set of microcracks (see Fig. A2) with arrays of continuously distributed edge dislocation, and supposing $a_k = 1$ without loss of the generality, a singular integral formulation for the macrocrack is

$$\sigma_{nn}^{(ma)}(\eta) + i\sigma_{in}^{(ma)}(\eta) = \int_{-\infty}^{0} \frac{2}{\eta - \xi} \bar{B}^{(ma)}(\xi)\, d\xi + \sum_{j=1}^{M} \int_{-1}^{1} [H_1 B^{(j)}(\xi) + H_2 \bar{B}^{(j)}(\xi)]\, d\xi \tag{A3}$$

where the superscript (ma) and (j) indicate the variables associated with the macrocrack and j-th microcrack respectively. To make the transform

$$\eta = \frac{u-1}{u+1}, \quad (-1 < u < 1) \quad \xi = \frac{t-1}{t+1}, \quad (-1 < t < 1) \tag{A4}$$

for the macrocrack as treated for the semi-infinite crack by Hutchinson *et al.* (1987), the formulation (A3) can be put into a suitable form for the numerical solution as follows

$$\sigma_{nn}^{(ma)}(u) + i\sigma_{in}^{(ma)}(u) = \int_{-1}^{1} \frac{h(u,t)}{u-t} \bar{B}^{(ma)}(t)\, dt + \sum_{j=1}^{M} \int_{-1}^{1} [H_1(u,\xi) B^{(j)}(\xi) + H_2(u,\xi) \bar{B}^{(j)}(\xi)]\, d\xi \tag{A5}$$

where

$$h(u,t) = \frac{2(u+1)}{t+1} \quad H_1(u,\xi) = \frac{2i\mathrm{Im}(z_j^{(ma)} - s)}{(z_j^{(ma)} - s)^2}, \quad H_2(u,\xi) = 2\mathrm{Re}\left(\frac{1}{z_j^{(ma)} - s}\right)$$

$$z_j^{(ma)} = (z_0^{(ma)} - c^{(j)}) + \frac{u-1}{u+1}, \quad s = (z_0^{(j)} - c^{(j)}) + \xi\, e^{i\theta_j}.$$

Similarly, the formulation for each microcrack can be given by

$$\sigma_{nn}^{(k)}(\eta_k) + i\sigma_{in}^{(k)}(\eta_k) = \int_{-1}^{1} \frac{h^{(k)}}{\eta_k - \xi} \bar{B}^{(k)}(\xi)\, d\xi + \sum_{\substack{j=1 \\ j \neq k}}^{M} \int_{-1}^{1} [G_1(\eta_k,\xi) B^{(j)}(\xi) + G_2(\eta_k,\xi) \bar{B}^{(j)}(\xi)]\, d\xi$$

$$+ \int_{-1}^{1} [F_1(\eta_k,t) \bar{B}^{(ma)}(t) + F_2(\eta_k,t) \bar{B}^{(ma)}(t)]\, dt \quad (k = 1,2,\ldots,M) \tag{A6}$$

where $h^{(k)} = 2e^{i\theta_k}$, the kernel functions G_1, G_2, F_1, F_2 are regular within $(-1, 1)$ and formulated as the following

$$G_1(\eta_k,\xi)=\frac{2ie^{2i\theta_k}\mathrm{Im}(z_j^{(k)}-s)}{(z_j^{(k)}-s)^2}+\frac{1-e^{2i\theta_k}}{z_j^{(k)}-s}\quad G_2(\eta_k,\xi)=2e^{2i\theta_k}\mathrm{Re}\left(\frac{1}{z_j^{(k)}-s}\right)+\frac{1-e^{2i\theta_k}}{\bar{z}_j^{(k)}-\bar{s}}$$

$$z_j^{(k)}=(z_0^{(k)}-c^{(j)})+\eta_k e^{i\theta_k},\quad s=(z_0^{(j)}-c^{(j)})+\xi e^{i\theta_j}$$

and

$$F_1(\eta_k,t)=\frac{2}{(1+t)^2}\left[\frac{2ie^{2i\theta_k}\mathrm{Im}(z_{ma}^{(k)}-s)}{(z_{ma}^{(k)}-s)^2}+\frac{1-e^{2i\theta_k}}{z_{ma}^{(k)}-s}\right]\quad F_2(\eta_k,t)=\frac{2}{(1+t)^2}\left[2e^{2i\theta_k}\mathrm{Re}\left(\frac{1}{z_{ma}^{(k)}-s}\right)+\frac{1-e^{2i\theta_k}}{\bar{z}_{ma}^{(k)}-\bar{s}}\right]$$

$$z_{ma}^{(k)}=(z_0^{(k)}-c^{(ma)})+\eta_k e^{i\theta_k},\quad s=(z_0^{(ma)}-c^{(ma)})+\frac{t-1}{t+1}$$

According to the relation between the relative crack displacements and the dislocation distribution, the behaviors of $B^{(ma)}$ as $t\to 1^-$ ($\xi\to 0^-$) and $t\to -1^+$ ($\xi\to\infty$) can be specified by the macrocrack tip field. The results are given below

$$\lim_{t\to 1^-} B^{(ma)}(t)=\frac{\bar{K}}{2\pi\sqrt{\pi}\sqrt{1-t}}\quad \lim_{t\to -1^+} B^{(ma)}(t)=\frac{\bar{K}^{\infty}\sqrt{1+t}}{4\pi\sqrt{\pi}} \tag{A7}$$

The alternative expressions are

$$K=(2\pi)^{3/2}\lim_{t\to 1^-}\sqrt{\frac{1-t}{1+t}}\,\overline{B^{(ma)}(t)}\quad K^{\infty}=(2\pi)^{3/2}\lim_{t\to -1^+}\sqrt{\frac{1-t}{1+t}}\,\overline{B^{(ma)}(t)} \tag{A8}$$

where K^{∞} is the known complex SIF to describe the remote field, and K is the complex SIF for the macrocrack tip. By considering the eqn (A7), $B^{(ma)}$ is taken to be

$$B^{(ma)}(t)=\sqrt{\frac{1+t}{1-t}}\sum_{m=0}^{\infty}\alpha_m^{(ma)}T_m(t) \tag{A9}$$

where $T_m(t)$ is the Chebyshev polynominal of the first kind of degree m, and $\alpha_m^{(ma)}$ is the complex coefficients.

It can be proved that $B^{(j)}$ for the j-th in microcrack can be expanded as (Erdogan *et al.*, 1973)

$$B^{(j)}(t)=\frac{1}{\sqrt{1-t^2}}\sum_{m=1}^{\infty}\alpha_m^{(j)}T_m(t)\quad (j=1,\ldots,M) \tag{A10}$$

which automatically satisfies the uniqueness of displacements, i.e.

$$\int_{-1}^{1}B^{(j)}(\xi)\,d\xi=0 \tag{A11}$$

After eqns (A9) and (A10) are substituted into eqns (A5), (A6) and (A8b), the known remote field and the boundary conditions that are traction free on the macrocrack as well as the traction distribution $p_k(\eta_k)$ on the microcracks are transformed into a group of singular integral equations

$$\sigma_{nn}^{(ma)}(u)+i\sigma_{tn}^{(ma)}(u)=0\quad \sigma_{nn}^{(k)}(\eta_k)+i\sigma_{tn}^{(k)}(\eta_k)=p_k(\eta_k)\quad (k=1,\ldots,M)\quad K^{\infty}=(2\pi)^{3/2}\sum_{m=0}^{\infty}(-1)^m\bar{\alpha}_m^{(ma)} \tag{A12}$$

By the aid of the numerical method for singular integral equation (Erdogan *et al.*, 1973), the coefficients $\alpha_m^{(ma)}$ in

eqn (A9) and $\alpha_m^{(l)}$ in eqn (A10) are obtained from eqn (A12). As consequence, SIF of the macrocrack can be calculated from eqn (A8a) without any difficulty, and is

$$K = (2\pi)^{3/2} \sum_{m=0}^{\infty} \bar{\alpha}_m^{(ma)} \tag{A13}$$

By the way, if the expansions (A9) and (A10) are substituted into eqns (A5), (A6) together with the equality

$$h(u,t)\bar{B}^{ma}(t) = \frac{2(u+1)}{\sqrt{1-t^2}} \sum_{m=0}^{\infty} \bar{\alpha}_m^{ma} T_m(t) \tag{A14}$$

the singular characteristic in eqn (A5) for macrocracks is the same as one in eqn (A6) for microcracks. Therefore, the procedure of the numerical solution for both equations is similar.